J|A|C|S
ARTICLES
Published on Web 01/19/2002

Calix[6]arene-Based Cuprous "Funnel Complexes": A Mimic for the Substrate Access Channel to Metalloenzyme Active Sites

Yannick Rondelez,[†] Marie-Noëlle Rager,[‡] Arthur Duprat,[§] and Olivia Reinaud*[,†]

Contribution from the Laboratoire de Chimie et Biochimie Pharmacologiques et Toxicologiques, CNRS UMR 8601, Université René Descartes, 45 rue des Saints-Pères, 75270 Paris Cedex 06, France, Service de RMN, CNRS UMR 7576, École Nationale Supérieure de Chimie de Paris (ENSCP), 11 rue Pierre et Marie Curie, 75231 Paris Cedex 05, France, and Laboratoire de Recherches Organiques associé au CNRS, École Supérieure de Physique et Chimie Industrielles de la Ville de Paris (ESPCI), 10 rue Vauquelin, 75231 Paris Cedex 05, France

Received May 15, 2001

Abstract: Two calixarene-based model systems (**a** and **b**) for monocopper enzymes are compared. Both present a tris(pyridine) coordination site for Cu that mimics the imidazole-rich neutral binding site in enzymes. Upon reaction with 1 equiv of copper(I), the tridentate ligands gave rise to ill-defined unsymmetrical complexes. However, in the presence of an organonitrile RCN (R = Me, Et, Ph), tetrahedral species were obtained, with the nitrilo ligand included in the calixarene hydrophobic cone. System **b** presents a larger cavity than system **a**, with a wider opening thanks to the removal of three *t*Bu groups from the calixarene structure. As a result, the recognition pattern for MeCN vs PhCN is inverted, and the relative affinity constants differ by 3 orders of magnitude. The mechanism of the acetonitrile exchange at the cuprous centers was studied by ^{1}H NMR spectroscopy. Thermodynamic and kinetic data show that it follows a dissociative pathway in both cases. The main differences between systems **a** and **b** stem from the presence of a door that entraps the guest in case **a**. In system **b** indeed, the removal of three calixarene *t*Bu groups led to a 100-fold acceleration of the MeCN exchange rate. Hence, these supramolecular systems provide a rare and interesting model for the hydrophobic substrate channel giving access to a metalloenzyme active site.

Introduction

A key step that needs to be completed in metalloenzyme mimics is to design a ligand that can reproduce the biocoordination sphere of the metal ion. However, the catalytic efficiency of these biomolecules stems from a combination of the well-suited electronic properties of the metallic site and the structural properties of the organic pocket in which it is buried.[1,2] Indeed, most of the selectivity results from the shape of this cavity and the chemical properties of the amino acids that define it. Hydrophobic amino acids, for example, are often found when the substrate is a nonpolar organic molecule.[2] Whereas a number of research groups have designed models aimed at reproducing the biological coordination core of the metal ion,[3−5] others have studied the noncovalent binding of organic guest into cavities.[6−11] Very few chemical models, however, include these two features simultaneously.[12,13] We have previously described copper[14−17] and zinc[18] complexes based on selectively functionalized calix-

* To whom correspondence should be addressed. E-mail: reinaud@biomedicale.univ-paris5.fr.
[†] Université René Descartes.
[‡] École Nationale Supérieure de Chimie de Paris (ENSCP).
[§] École Supérieure de Physique et Chimie Industrielles de la Ville de Paris (ESPCI).

(1) (a) Holm, R. H.; Kennepohl, P.; Solomon, E. I. *Chem. Rev.* **1996**, *96*, 2239−2314. (b) Lippard, S. J.; Berg, J. M. *Principles of Bioinorganic Chemistry*; University Science Books: Mill Valley, CA, 1994. (c) Cowan, J. A. *Inorganic Biochemistry, an Introduction*; Wiley-VCH: New York, 1997. (d) Bertini; Gray; Lippard; Valentine *Bioinorganic Chemistry*; University Science Books: Mill Valley, CA, 1994. (e) Kaim, W.; Rall, J. *Angew. Chem., Int. Ed. Engl.* **1996**, *35*, 43−60.
(2) *Cytochrome P450, Structure, Mechanism, and Biochemistry*; Plenum Press: New York, 1995.
(3) (a) Ibers, J. A.; Holm, R. H. *Science* **1980**, *209*, 223−235. (b) Karlin, K. D. *Science* **1993**, *261*, 701−708. (c) Messerschmidt, A. Metal Sites in Proteins and Models. In *Structure and Bonding*, Vol. 90; Hill, H. A. O., Sadler, P. J., Thomson, A. J., Eds.; Springer-Verlag: Berlin-Heildelberg, 1998; pp 37−68. (d) Fenton, D. E. *Chem. Soc. Rev.* **1999**, *28*, 159−168.
(4) For recent examples on copper enzymes modeling, see: (a) Decker, H.; Dillinger, R.; Tuczek, F. *Angew. Chem., Int. Ed.* **2000**, *39*, 1591−1595. (b) Chen, P.; Fujisawa, K.; Solomon, E. I. *J. Am. Chem. Soc.* **2000**, *122*, 10177−10193. (c) Blain, I.; Giorgi, M.; de Riggi, I.; Réglier, M. *Eur. J. Inorg. Chem* **2001**, 205−211.
(5) Calix[4]arenes have been used as platforms for the preorganization of copper binding sites in dinuclear Cu enzyme models. See: (a) Molenveld, P.; Engbersen, J. F. J.; Reinhoudt, D. N. *Chem. Soc. Rev.* **2000**, *29*, 75−86. (b) Xie, D.; Gutsche, C. D. *J. Org. Chem.* **1998**, *63*, 9270−9278.
(6) (a) Schneider, H.-J. *Angew. Chem., Int. Ed. Engl.* **1991**, *30*, 1417−1436. (b) Reviews of Molecular Recognition. *Chem. Rev.* **1997**, *97*, 1232−1734 (special issue). (c) Reviews of Cyclodextrins. *Chem. Rev.* **1998**, *98*, 1741−2076 (special issue). (d) Davis, A. P.; Wareham, R. S. *Angew. Chem., Int. Ed. Engl.* **1989**, *28*, 2978−2996. (e) Lehn, J. M. *Supramolecular Chemistry*; VCH: Weinheim, 1995. (f) Cram, D. J.; Cram, J. M. *Container Molecules and Their Guests, Monographs in Supramolecular Chemistry*; The Royal Society of Chemistry: Cambridge, 1994.
(7) (a) Gutsche, C. D. *Calixarenes, Monographs in Supramolecular Chemistry*; The Royal Society of Chemistry: Cambridge, 1989. (b) Gutsche, C. D. *Calixarenes Revisited, Monographs in Supramolecular Chemistry*; The Royal Society of Chemistry: Cambridge, 1998. (c) Arduini, A.; Secchi, A.; Pochini, A. *J. Org. Chem.* **2000**, *65*, 9085−9091.
(8) Collet, A. *Tetrahedron* **1987**, *43*, 5725−5759.
(9) Breslow, R.; Dong, S. D. *Chem. Rev.* **1998**, *98*, 1997−2011.
(10) Rudkevich, D. M.; Rebek, J., Jr. *Eur. J. Org. Chem.* **1999**, 1991−2005.
(11) Herm, M.; Schrader, T. *Chem. Eur. J.* **2000**, *6*, 47−53.

10.1021/ja0161958 CCC: $22.00

[6]arenes. In these systems, three nitrogen arms fix the metal center, leaving a free coordination site situated inside a hydrophobic pocket. The calixarene cavity, constrained in a cone conformation, acts as a selective molecular funnel for neutral molecules. These biomimetic complexes maintain a high degree of flexibility,[16] which is known to be essential in natural systems, in particular for fast substrate access and product departure.[2,19] The present work focuses on the importance of the cavity.

Pyridine groups are often used to model the nitrogen-rich binding site of copper in enzymes.[20−22] We have previously shown that calixarene **2a**, presenting three pyridine groups, is capable of stabilizing a mononuclear cuprous center whose interactions with exogeneous ligands are controlled by the calixarene cavity (Scheme 1). As a consequence, although resistant to air autoxidation, the Cu(I) complex behaves as a receptor, presenting a good affinity for small nitriles RCN (R = Me, Et, allyl).[14] To evaluate the importance of the role of the cavity, we have now synthesized a slightly modified ligand, **2b**, where three out of the six calixarene *t*Bu substituents were removed. The new ligand **2b** offers a larger pocket with a wider opening than **2a**. We studied the comparative binding of different nitriles to these two calixarene-based mononuclear Cu(I) centers (**3a** and **3b**) by ^{1}H NMR spectroscopy. In this paper, we show how modification of the cavity size and shape allows for the fine-tuning of the thermodynamic and kinetic features of supramolecular biomimetic Cu systems.

Results

Synthesis. The tris(methyl)ether derivative of *t*Bu-calix[6]-arene **1a** was reacted with $AlCl_3$ in order to selectively remove the *t*Bu substituents on the phenol groups.[23] The resulting compound **1b** was subsequently alkylated with 2-picolyl chloride to provide ligand **2b** with a good yield. ^{1}H NMR analysis of this new ligand showed only one broad singlet for the bridging CH_2 protons of the calixarene structure. This stands in contrast to ligand **2a**, for which two doublets were observed for the same group of protons,[14] and shows that the exchange process between the two equivalent C_3 cone conformations is faster for **2b** than for **2a**. Indeed, it is well known that the cone−cone interconversion can take place via both a "*t*Bu or a phenoxy through the annulus" pathway. For compound **2b**, a preferred "de-*tert*-butylated through the annulus" pathway probably occurs, thereby attesting to its higher flexibility.

Scheme 1. Synthesis of the Biomimetic Supramolecular Calix[6]arene-Based Cuprous Systems Presenting Two Different Cavities[a]

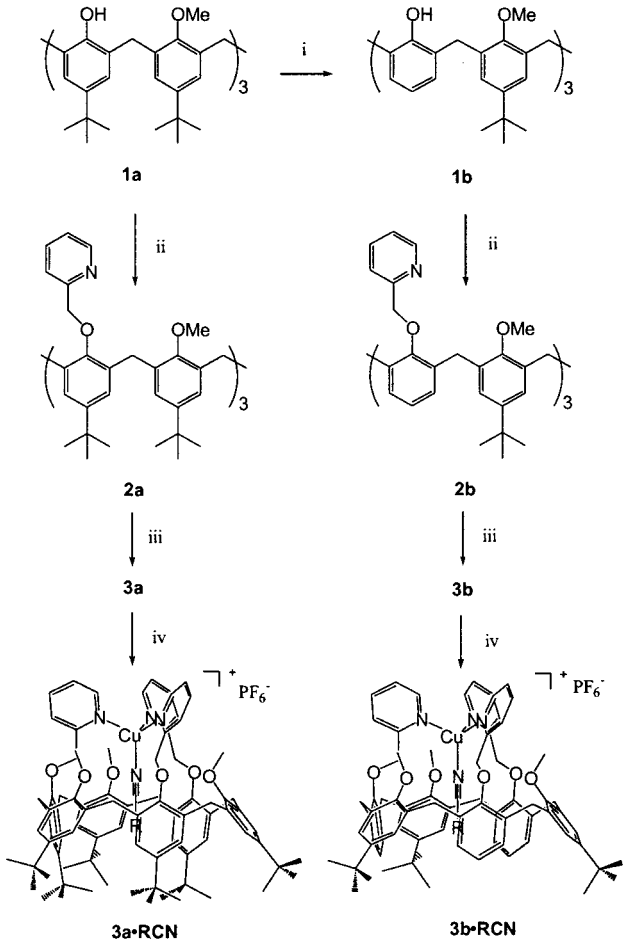

[a] Reagents and conditions: (i) $AlCl_3$, toluene; (ii) 2-chloromethylpyridine, NaH, THF; (iii) $Cu(NCMe)_4PF_6$, THF; (iv) CD_2Cl_2, RCN.

Both ligands were reacted with a stoichiometric equivalent of $Cu(NCMe)_4PF_6$ in THF. The corresponding cuprous complexes **3a** and **3b** were isolated by precipitation with pentane. This procedure yielded complexes that were free of MeCN and presented a good solubility, even in noncoordinating solvents. The 1:1 Cu/ligand ratio was confirmed by elemental analyses.[24]

In CD_2Cl_2 solution at room temperature, complexes **3** showed ill-defined and broad ^{1}H NMR spectra. By lowering the

(12) In reviews specifically oriented toward supramolecular chemistry of transition metal complexes, only a few references concern this aspect. See: (a) Linton, B.; Hamilton, A. D. *Chem. Rev.* **1997**, *97*, 1669−1680. Sanders, J. K. M. *Chem. Eur. J.* **1998**, *4*, 1378−1383. (b) Feiters, M. C. Supramolecular Catalysis. In *Comprehensive Supramolecular Chemistry*, Vol. 10; Reinhoudt, D. N., Ed.; Pergamon: New York, 1996; pp 267−360. (c) Murakami, Y.; Kikuchi, J.-I.; Hisaeda, Y.; Hayashida, O. *Chem. Rev.* **1996**, *96*, 721−758. (d) Feiters, M. C.; Klein Gebbink, R. J. M.; Schenning, A. P. H. J.; van Strijdonck, G. P. F.; Martens, C. F.; Nolte, R. J. M. *Pure Appl. Chem.* **1996**, *68*, 2163-2170. (e) Rizzarelli, E.; Vecchio, G. *Coord. Chem. Rev.* **1999**, *188*, 343−364.
(13) Recent examples: (a) Breslow, R.; Zhang, X.; Huang, Y. *J. Am. Chem. Soc.* **1997**, *119*, 4535−4536. (b) Rybak-Akimova, E. V.; Kuczera, K.; Jas, G. S.; Deng, Y.; Busch, D. H. *Inorg. Chem.* **1999**, *38*, 3423−3434. (c) Elemans, J. A. A. W.; Claase, M. B.; Aarts, P. P. M.; Rowan, A. E.; Schenning, A. P. H. J.; Nolte, R. J. M. *J. Org. Chem.* **1999**, *64*, 7009−7013. (d) French, R. R.; Holzer, P.; Leuenberger, M. G.; Woggon, W.-D. *Angew. Chem., Int. Ed.* **2000**, *39*, 1267−1269.
(14) Blanchard, S.; Le Clainche, L.; Rager, M.-N.; Chansou, B.; Tuchagues, J.-P.; Duprat, A. F.; Mest, Y.; Reinaud, O. *Angew. Chem., Int. Ed.* **1998**, *37*, 2732−2735.
(15) Le Clainche, L.; Giorgi, M.; Reinaud, O. *Inorg. Chem.* **2000**, *39*, 3436−3437.
(16) Rondelez, Y.; Sénèque, O.; Rager, M.-N.; Duprat, A.; Reinaud, O. *Chem. Eur. J.* **2000**, *6*, 4218−4226.
(17) Le Clainche, L.; Rondelez, Y.; Sénèque, O.; Blanchard, S.; Campion, M.; Giorgi, M.; Duprat, A. F.; Mest, Y.; Reinaud, O. *C. R. Acad. Sci., Chimie, Série IIc* **2000**, *3*, 811−819.
(18) (a) Sénèque, O.; Rager, M.-N.; Giorgi, M.; Reinaud, O. *J. Am. Chem. Soc.* **2000**, *122*, 6183−6189. (b) Sénèque, O.; Giorgi, M.; Reinaud, O. *J. Chem. Soc.*, **2001**, *123*, 8442−8443. Chem. Commun. **2001**, 984−985.
(19) Frieden, E. *J. Chem. Educ.* **1975**, *52*, 754−761.
(20) Szczepura, L. F.; Witham, L. M.; Takeuchi, K. J. *Coord. Chem. Rev* **1998**, *174*, 5−32.
(21) Jonas, R. T.; Stack, T. P. D. *Inorg. Chem.* **1998**, *37*, 6615−6629.
(22) For reviews concerning copper enzymes models, see: (a) Kitajima, N.; Moro-oka, Y. *Chem. Rev.* **1994**, *94*, 737−757. (b) Karlin, K. D.; Kaderli, S.; Zuberbühler, A. D. *Acc. Chem. Res.* **1997**, *30*, 139−147. (c) Mahadevan, V.; Gebbink, R. J. M. K.; Stack, T. D. P. *Curr. Opin. Chem. Biol.* **2000**, *4*, 228−234. (d) Blackman, A. G.; Tolman, W. B. Metal-Oxo and Metal-Peroxo Species in Catalytic Oxidations. In *Structure and Bonding*, Vol. 97; Meunier, B., Ed.; Springer-Verlag: Berlin Heidelberg, 2000; pp 179−211.
(23) van Duynhoven, J. P. M.; Janssen, R. G.; Verboom, W.; Franken, S. M.; Casnati, A.; Pochini, A.; Ungaro, R.; de Mendoza, J.; Nieto, P. M.; Prados, P.; Reinhoudt, D. N. *J. Am. Chem. Soc.* **1994**, *116*, 5814−5822.
(24) When the complexation step was effected with MeCN as a cosolvent, the acetonitrilo ternary complex was isolated (see ref 14).

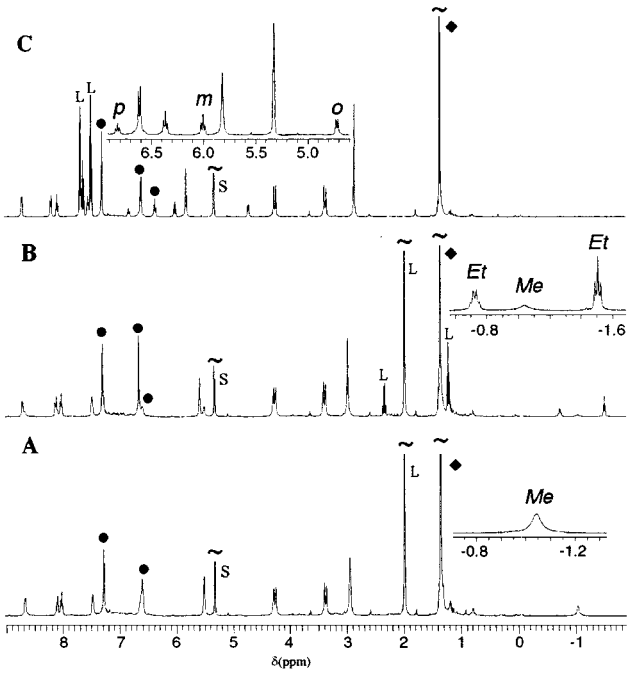

Figure 1. ^{1}H NMR spectra of complexes **3b·RCN** in CD_2Cl_2 at 243 K (400 MHz). [**3b**] = 10 mM. (A) [MeCN] = 50 mM; (B) [MeCN] = 50 mM and [EtCN] = 17 mM; (C) [PhCN] = 60 mM. Resonances for the free nitriles RCN are labeled L. The solvent peak is labeled S. Host's aromatic and *tert*-butyl protons are labeled ● and ◆, respectively. Regions showing the resonances for the coordinated RCN have been enlarged. Similar profiles were obtained for complexes **3a·RCN** (spectra not displayed).

temperature, the profiles were sharpened, but they nonetheless remained complicated, attesting to a complete lack of symmetry. This may be due to the coordination of only two pyridine arms[25] and/or related to problems of cavity filling. Indeed, the addition of an organonitrile RCN dramatically changed the NMR pattern, attesting to the formation of new species, of which a detailed study is presented below.

Thermodynamics. In a 50 mM MeCN solution in CD_2Cl_2, complexes **3** (10 mM) gave rise, in each case, to a new species as shown by the ^{1}H NMR analyses. Although broad, the NMR profiles presented a reduced number of peaks that was consistent with C_3 symmetry.[26] Raising the temperature to 308 K led the spectra to broaden. In contrast, they sharpened on lowering the temperature (Figure 1A), and a new resonance at ca. $\delta = -1.1$ ppm was observed. This is characteristic of the formation of tetrahedral complexes **3·MeCN** with a bound MeCN in the shielded environment of the calixarene cavity. Adding propionitrile to the same NMR tubes did not significantly modify the overall spectra, except in the high-field region. A quadruplet and a triplet appeared at ca. −0.8 and −1.6 ppm, respectively, attesting to the competitive coordination of propionitrile inside the cavity (Figure 1B). More interestingly, upon addition of benzonitrile to solutions of **3** that were free of other nitriles, the benzonitrilo complexes **3·PhCN** were observed at 243 K with two triplets and one doublet in the 6.8−4.8 ppm region of the NMR spectra (Figure 1C).

Table 1. Equilibrium Constants $K_{RCN/MeCN}$ Measured at 243 K for the Ligand Exchange (**RCN** vs **MeCN**) at the Cu^+ Center in the Cavity of Calixarenes **a** and **b**

host	$K_{EtCN/MeCN}$	$K_{PhCN/MeCN}$
3a	5.6(5)	0.002(1)
3b	13(3)	2.1(5)

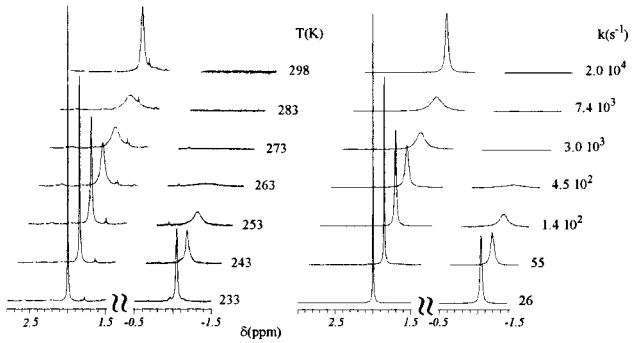

Figure 2. Temperature variation of the ^{1}H NMR spectra of the acetonitrile ($MeCN_{free}$ and $MeCN_{bound}$) regions of complex **3b·MeCN** in CD_2Cl_2 (left) and the corresponding computer-simulated spectra using the program g-NMR (right). Experimental conditions: $[\mathbf{3b}]_{initial} = 10$ mM and $[MeCN]_{initial} = 50$ mM. Similar profiles were obtained for complex **3a·MeCN** (spectra not displayed).

From guest competition experiments and integration of the ^{1}H NMR spectra obtained at 243 K, we measured the equilibrium constants $K_{RCN/MeCN}$ (Table 1) defined for the following equilibrium:

$$\mathbf{3{\cdot}MeCN} + \mathrm{RCN} \rightleftarrows \mathbf{3{\cdot}RCN} + \mathrm{MeCN} \quad (\text{with R} = \text{Et, Ph})$$

$$K_{RCN/MeCN} = [\mathbf{3{\cdot}RCN}][MeCN]/[\mathbf{3{\cdot}MeCN}][RCN]$$

For **3a**, the decreasing order of affinity is EtCN > MeCN ≫ PhCN. Hence, the affinity of the cuprous center for small ligands such as acetonitrile and propionitrile is ca. 3 orders of magnitude higher than for benzonitrile.[27] Complex **3b** exhibited a completely different behavior since the affinity order became EtCN > PhCN > MeCN. In this novel system, the host prefers benzonitrile over acetonitrile by a factor of 2.

Ligand Exchange. We undertook a comparative kinetic study for the acetonitrile exchange process in systems **3·MeCN**. Both complexes displayed similar behavior with, however, a temperature difference of 30 K. MeCN exchange at the metal center took place at a rate close to the NMR analysis time scale. The resonance corresponding to free acetonitrile ($MeCN_{free}$) was broad at 293 K and narrowed when the temperature was lowered. Whereas the peak for the included MeCN ($MeCN_{bound}$) was observable at 293 K for a 10 mM solution of complex **3a·MeCN** in CD_2Cl_2, it was detectable only below 263 K for system **b**. The exchange rate constants ($MeCN_{bound} \rightarrow MeCN_{free}$) were obtained by simulation of the corresponding resonances (Figure 2). An Eyring plot (shown in Figure 3) yielded the activation parameters $\Delta H^{\ddagger}$ and $\Delta S^{\ddagger}$ reported in Table 2.

As the temperature was raised, the ratio $MeCN_{bound}/MeCN_{free}$ decreased, suggesting that an intermediate species that is

(25) This phenomenon has been frequently observed for copper(I) complexes with tri- or tetradentate nitrogen-containing chelates. See: Liang, H.-C.; Karlin, K. D.; Dyson, R.; Kaderli, S.; Jung, B.; Zuberbühler, A. D. *Inorg. Chem.* **2000**, *39*, 5884−5894 and references cited therein.

(26) At 298 K, the spectrum of **3b** (10 mM) in CD_2Cl_2 was extremely broad. Upon addition of acetonitrile (300 mM), it became sharper, but the improvement was not as spectacular as for **3a**, and the peaks remained quite broad. Contrary to **3a**, no extra resonance could be detected in the high-field region at this temperature.

(27) As previously described (see ref 14), when the starting material is the acetonitrile adduct **3a·MeCN**, formation of **3a·PhCN** is hardly detectable upon addition of 20 molar equiv of PhCN to a 10 mM solution.

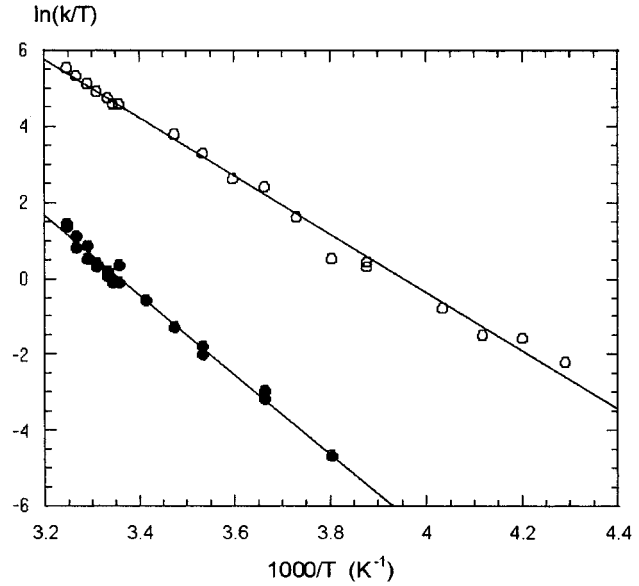

Figure 3. Eyring plots for the MeCN exchange at the Cu(I) center in complexes **3·MeCN** in CD_2Cl_2. Filled circle, system **a**; open circles, system **b**. Experimental conditions: $[\mathbf{3a}]_{initial} = 10$ mM and [MeCN] = 55 mM (5.5 equiv) or $[\mathbf{3a}]_{initial} = 20$ mM and [MeCN] = 60 mM (3 equiv); $[\mathbf{3b}]_{initial} = 10$ mM and [MeCN] = 50 or 75 mM (5 or 7.5 MeCN equiv). For more details on the NMR analyses and calculations, see the Supporting Information.

Table 2. Estimated Activation and Thermodynamic Parameters and Calculated Rate Constants for the MeCN Exchange Process in Complexes **3·MeCN** in CD_2Cl_2 ($MeCN_{bound} \rightarrow MeCN_{free}$)

	k_{298} (s^{-1})	$\Delta H^{\ddagger}$ (kJ mol^{-1})	$\Delta S^{\ddagger}$ (J K^{-1} mol^{-1})	ΔH (kJ mol^{-1})	ΔS (J K^{-1} mol^{-1})
3a	3.0×10^2(5)	86(3)	94(5)	72(6)	210(30)
3b	2.8×10^4(5)	64(2)	54(3)	41(4)	130(20)

acetonitrile-free was accumulating. Although not directly measurable from the integrated spectra, its concentration was obtained by deduction from the curve fittings. As it was found independent of the water concentration, we can assume that in this intermediate species, H_2O does not coordinate the cuprous center.

Therefore, we propose the following equilibrium, which is substantiated by the van't Hoff plots displayed in Figure 4:

$$\mathbf{3{\cdot}MeCN} \rightleftarrows \mathbf{3} + \text{MeCN}$$

$$K = [\mathbf{3}][\text{MeCN}]/[\mathbf{3{\cdot}MeCN}]$$

The thermodynamic parameters are given in Table 2.

Discussion

Folding. It is important to note that the well-defined C_3 cone conformation of the calixarene host is stabilized only in the presence of a coordinating guest. In the absence of any exogenous ligand, hosts **3** do not adopt a symmetrical conformation. This may well be related to the problem of cavity filling. Indeed, the calixarene, which is a highly flexible molecule, has a strong tendency to adopt a conformation well suited to optimize the interactions of its aromatic moieties with other groups. We have previously shown that when the coordinating guest is too small to fill the cavity, the latter autoincludes one of its *t*Bu substituents, thereby optimizing its filling.[28] In the case of systems **3**, the presence of an exogenous ligand at the cuprous center is necessary to organize the calixarene structure into a cavity. The π-basic pocket then wraps itself around the apical organic ligand, arriving at its symmetrical conformation.

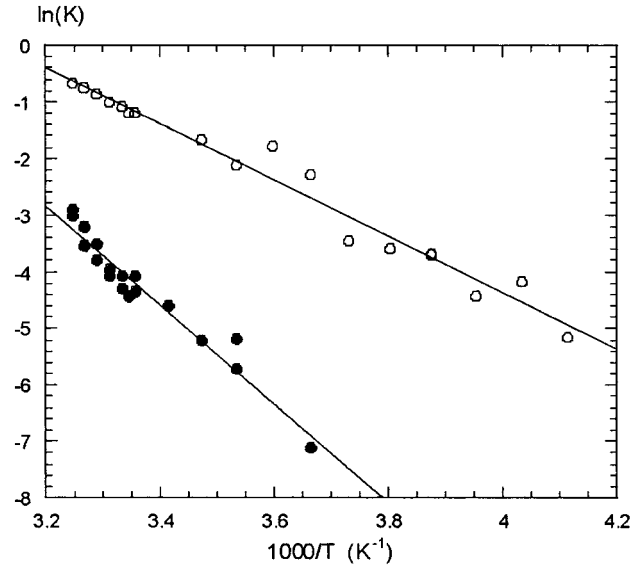

Figure 4. Van't Hoff plots for the equilibria **3·MeCN** ⇄ **3** + MeCN in CD_2Cl_2. Solid circles, system **a**; open circles, system **b**. See Figure 3 for experimental conditions.

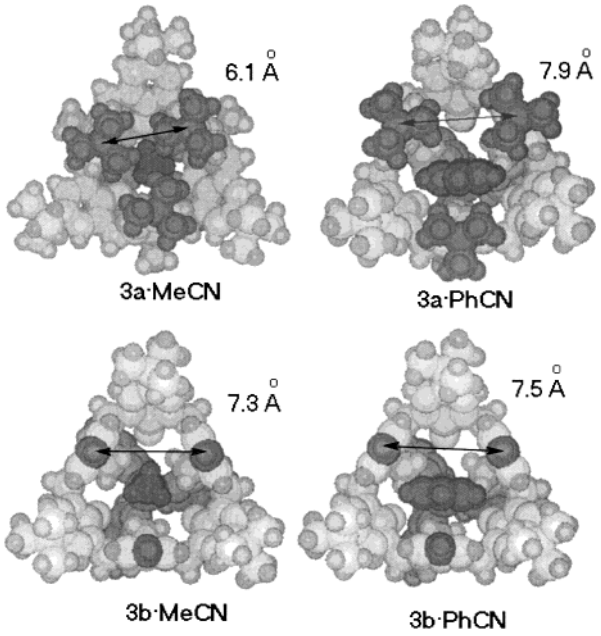

Figure 5. Comparison of the energy-minimized structures of the calixarene-based Cu(I) complexes.[31] The bottom views show the entrance of the cavities. The indicated distances correspond to the average basis of the triangles defined by the three closest para aromatic carbons.

Conformation. As previously demonstrated in the case of **3a·MeCN**,[14] the *t*Bu groups lie alternatively in *in* and *out* positions relative to the cavity. Those attached to the anisole groups stand outside. The others are stacked next to the C_3 axis, closing the entrance of the calixarene funnel (Figure 5 top left). Hence, the $t\text{Bu}_{in}$ groups are the natural targets for any attempt to open the cavity. This led us to synthesize system **b**.

(28) We previously described a closely related calixarene-based CuCO complex that underwent "a three-step dance" with a *t*Bu group partially included in the calixarene cavity, to compensate the smallness of the CO guest. See ref 16.

Table 3. Comparison of Some ^{1}H NMR δ Shifts (in CD_2Cl_2 at 243 K) in Complexes **3·RCN** for Hosts **a** and **b** with Three Different Guests[a]

	3a·MeCN	3a·EtCN	3a·PhCN	3b·MeCN	3b·EtCN	3b·PhCN
$\delta(ArH_{in})$	6.69	6.74	7.02	6.61	6.65	6.61
$\delta(t\text{Bu}_{in})$	0.72	0.77	0.94			
$\delta(ArH_{out})$	7.34	7.35	7.25	7.28	7.30	7.30
$\delta(t\text{Bu}_{out})$	1.37	1.37	1.20	1.35	1.35	1.35
$\delta(RCN_{bound})$	−1.16	−0.83 (q) −1.50 (t)	*o:* 4.88(d) *m:* 5.70(t) *p:* 6.60(t)	−1.05	−0.73(q) −1.50(d)	*o:* 4.72(d) *m:* 6.00(t) *p:* 6.82(t)

[a] Shifts are given in ppm.

The ^{1}H spectra of complexes **3·MeCN** recorded at 230 K are very similar. All groups of protons that coexist on both ligands display almost identical δ shifts. This indicates that the new complex **3b·MeCN** adopts the same conformation as **3a·MeCN**, with the remaining *t*Bu still occupying an *out* position. Computer modeling of the corresponding complexes, displayed in Figure 5 (bottom left), illustrates the opening of the cavity access when system **b** is substituted for system **a**, thereby showing that our initial goal had been reached.[29]

Host Flexibility. Interestingly, in complexes **3a·RCN,** the relative chemical shifts ArH_{in} vs ArH_{out} and $t\text{Bu}_{in}$ vs $t\text{Bu}_{out}$ are correlated to the size of the guest. For a small guest (R = Me), the difference in δ shifts for the *t*Bu groups is 0.65, whereas for a large one (R = Ph), it decreases to 0.26 (see Table 3).[30] This indicates that when the guest is larger, the alternate position of the calixarene aromatic units becomes less accentuated. As the large PhCN guest comes in, the *in* units move away from the C_3 axis and, like the swing of a pendulum, the *out* units come closer, leading to a less flattened and more conic conformation. Hence, the cavity shape adapts itself to the guest. In contrast, no significant difference in the host chemical shifts was observed when the guest size varied from MeCN to PhCN for **3b**. This suggests that the large PhCN guest does not distort cavity **b**.

These observations are fully corroborated by modeling studies. A comparison of the energy minimized structures of complexes **3·RCN** with R = Me and Ph is shown in Figure 5. The average distance between three equivalent *para* aromatic carbons of the calixarene ligands defines the base of two triangles. The *in* triangle is 1.8 Å wider for **3a·PhCN** than for **3a·MeCN**, whereas the *out* triangle is 1 Å narrower. On the other hand, for complexes **3b·RCN**, no significant change in conformation is visible upon replacement of MeCN by PhCN.

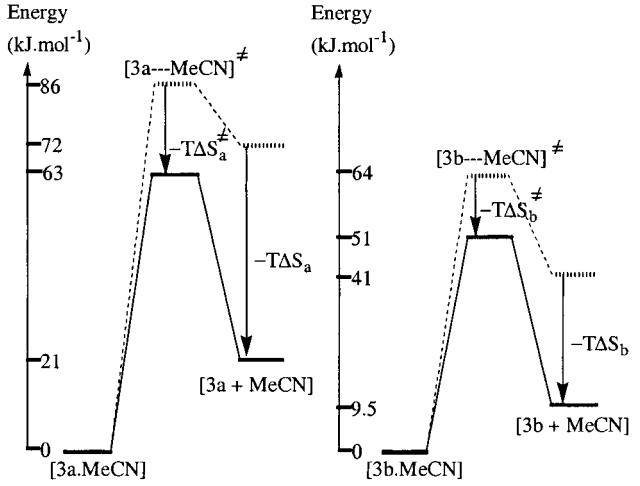

Figure 6. Energy diagrams for the MeCN dissociation at the cuprous center in system **3a** (left) and **3b** (right). Full line, ΔG(243 K); dotted line, ΔH.

Pocket Size and Shape. For both systems **a** and **b**, propionitrile appeared to provide the best fit for the calixarene pocket, leading to the highest affinity constant. Indeed, the guest flexibility probably allows its interactions with the host structure to be optimized. Most interesting is the striking difference in the relative affinity of systems **a** and **b** for MeCN and PhCN. The comparative results indicate a ratio of 1000 between the two $K_{PhCN/MeCN}$ constants. This large inversion factor can be explained by the fact that, in **3a**, the large guest "bumps" into the non-anisole *t*Bu that are in the *in* position. Removing these groups as in system **b** eliminates the corresponding energy cost, and the stabilizing interactions between the guest and the aromatic walls of the host then become the dominant factor.

Exchange Mechanism. The MeCN exchange rate was found to be first order in copper complex but independent of MeCN concentration. The corresponding values of the activation entropy $\Delta S^{\ddagger}$, reported in Table 2, are large and positive. These observations are consistent with a dissociative mechanism.[32] This allowed us to draw energy diagrams for the exchange processes in both systems **a** and **b**. In Figure 6, the Gibb's energy and enthalpy values were calculated for a temperature of 243 K.

Comparison of the thermodynamic parameters indicates that system **a** presents a stronger affinity for MeCN than system **b** does. Acetonitrile is, in fact, not a particularly good ligand for **3b**, and the equilibrium constant is close to 1 at room temperature. The energy diagrams show that the entropy gain

(29) This stands in contrast to the Zn complexes and will be discussed elsewhere.
(30) The pseudo-C_3 symmetry of complexes **3·PhCN** indicates that the guest ligand is spinning inside the cavity at a rate that is faster than the NMR analysis time scale. As a result, the anisotropy due to the aromatic nucleus of the guest is small.
(31) The calixarenes were sketched and optimized using the esff force field of the Biosym package Insight/Discover (Release 95.0, Biosym/MSI, San Diego, CA, 1995), on an IBM RISC 6K workstation. The RX structure of **3a·EtCN** described in ref 14 was used as a basis. The standard Discover 3 algorithms were selected with their default inputs (0.001 for BFGS Newton energy convergence). Due to the medium size of the molecules, no cutoff was used to compute the nonbond contribution. The Cu−N distances and N−Cu−N angles in model **3a**. EtCN distances were very similar to those found in the X-ray structure. No significant differences for these calculated values were observed for compounds **3·RCN** with various R groups in either system **a** or **b** (see Supporting Information). Significant modification of the Zn coordination core in a closely related system with MeCN vs EtCN as a guest ligand was not observed in the X-ray structures (see ref 18a and Sénèque, O.; Rondelez, Y.; Le Clainche, L.; Inisan, C.; Rager, M.-N.; Giorgi, M.; Reinaud, O. *Eur. J. Inorg. Chem.* **2001**, 2597−2604.). Hence, although geometrical factors may induce some electronic effects at the cuprous center (and in particular influence the Cu−NCR bond strength), these are probably small and do not play a major role in the observed selectivity for the RCN guests.
(32) Atwood, J. D. *Inorganic and Organometallic Reaction Mechanisms*, 2nd ed.; VCH Publishers: New York, 1997.

upon MeCN release is quite significant compared to the enthalpic cost. It is higher in system **a** than in system **b**, which may be due to the higher degree of order in the ternary species **3a·MeCN** induced by the alternate *t*Bu positioning. Likewise, a higher enthalpic difference ΔH_a compared to ΔH_b might well stem not from the difference in enthalpy between the four-coordinate complexes **3·MeCN**, but rather from the species **3**. Indeed, whereas the formers adopt similar conformations, there may well be a more stable conformation for the acetonitrile-free complex **3b** that is not accessible for the more sterically constrained **3a**.

MeCN dissociation involves three main processes that account for the energy barrier: (i) the $Cu-N_{nitrilo}$ bond break, (ii) the decrease of the stabilizing hydrophobic interactions between the guest ligand and the π-basic host, and (iii) the opening of the *t*Bu gate at the exit of the funnel. Table 2 shows both higher entropic and enthalpic costs for system **a**. However, as mentioned above, the electronic environment of Cu(I) and the conformation adopted by the host structures are similar in systems **a** and **b**. Therefore, the Cu−N bond strength and the stabilizing hydrophobic host/guest interactions are probably of the same order of magnitude.[33] A higher activation energy for the exchange in **3a·MeCN** compared to that in **3b·MeCN** is thus related to a more sterically constrained transition state (relative to the four-coordinated species). Therefore, we propose that the relative kinetic stability of **3a·MeCN** is due to the necessity of "opening the door" for the dissociating nitrile on its way out of cavity **a**. In other words, the gate constituted by the $t\text{Bu}_{in}$ groups traps the guest inside the calixarene cavity. This makes the transition state later, for even when the $Cu-N_{nitrilo}$ bond is partially broken, the guest still has to open the door.

An interesting analogy can be made with metalloenzymes, especially those involved in oxidative processes. The very well known cytochromes $P\text{-}450_{cam}$ and $P\text{-}450_{BM3}$ for example, present aromatic residues along the path of access.[2] The hydrophobic substrate diffuses from the molecular surface to the active site thanks to dynamic fluctuations of the residues forming the channel. As a result, the proteins must undergo a very large conformational change, leading to the opening/closure of the access channel which enables substrates to enter and bind. Indeed, site-directed mutagenesis experiments have shown that the rate of substrate release is highly dependent on the nature of the protein residues that line the channel. Similar hydrophobic channels have been observed in copper oxidases as well.[34]

Conclusions

Herein, we have described a model for the cuprous site of monocopper enzyme that is unique inasmuch as it provides not only a biomimetic N_3 neutral coordination site but also a cavity that controls the access to the metal center. The synthesis of a partially de-*tert*-butylated calix[6]arene ligand gave rise to a new system (**b**), offering a cavity of different size and shape than the fully *tert*-butylated one (**a**). The two calixarene-based systems present the same tris-pyridine neutral coordination core. Comparison of their respective cuprous complexes led to important information relative to the specific role of the cavity. Indeed, we showed that both thermodynamic and kinetic properties were greatly affected. The recognition pattern of the cuprous complexes for nitrilo ligands was inverted as the affinity of system **b** compared to that of system **a** for PhCN vs MeCN gained 3 orders of magnitude. The exchange process at the metal center was shown to be dissociative. The thermodynamic and kinetic parameters indicated that the main difference between these systems stems from the presence or absence of the gate formed by three *t*Bu groups trapping the coordinated MeCN ligand inside the cavity. Removing the door induced a 100-fold acceleration of the guest release. Hence, our system provides a nice model for the substrate channel giving access to the active site in metalloenzymes.

(33) The CH_3 group of MeCN is too far from the *t*Bu substituents to interact: *d*(C···C) between the methyl groups is 3.69 Å.
(34) See, for example: Chen, Z.; Schwartz, B.; Williams, N. K.; Li, R.; Klinman, J. P.; Mathews, F. S. *Biochemistry* **2000**, *39*, 9709−9717.

Experimental Section

General Procedures. All solvents and reagents were obtained commercially. THF was distilled over sodium/benzophenone under argon. ^{1}H and ^{13}C NMR spectra were recorded either on a Bruker Avance 400 or on a Bruker AC 200 spectrometer. Traces of residual solvent were used as an internal standard. Solid-state IR measurements (KBr pellets) were carried out on a Perkin-Elmer 783 IR spectrophotometer. Elemental analyses were performed at the Université Pierre et Marie Curie, France. For this purpose, the products were dried overnight under vacuum at 60−70 °C.

5,17,29-Tris-*tert*-butyl-37,39,41-trimethoxy-38,40,42-*tris*[(2-pyridyl)-methoxy]calix[6]arene (2b). Under an argon atmosphere, a mixture of **1b** (300 mg, 0.35 mmol), NaH (60% in oil, 425 mg, 11 mmol), and 2-chloromethylpyridine chlorhydrate (580 mg, 3.5 mmol) in dry THF (15 mL) was refluxed overnight. The solution was then concentrated and water carefully added. The brownish solid obtained was collected and then filtrated on SiO_2, using CH_2Cl_2/MeOH 98/2 as an eluant. Removal of the solvents under vacuum led to a colorless product (270 mg) in a 68% yield. Mp: 96 °C (decomp). ^{1}H NMR (200 MHz, $CDCl_3$, 298 K): δ 1.31 (27H, s, *t*Bu), 2.69 (9H, s, OCH_3), 4.02 (12H, bs, $Ar-CH_2-Ar$), 5.06 (6H, s, $Py-\alpha CH_2$), 6.71 (9H, bs, ArH_m and ArH_p), 7.20 (6H, s, ArH), 7.25 (3H, m, PyH), 6.76 (6H, m, PyH and PyH), 8.60 (3H, d, J = 4.6 Hz, PyH). ^{13}C NMR (50.0 MHz, $CDCl_3$, 298 K): δ 30.7 ($Ar-\alpha CH_2$), 31.6 ($C(CH_3)_3$), 34.2 ($C(CH_3)_3$), 60.1 (OCH_3), 75.0 ($Py-\alpha CH_2$), 121.4 ($C_{Py}H$), 122.5 ($C_{Py}H$), 123.8 ($C_{Ar}H$), 127.4 ($C_{Ar}H_m$ and $C_{Ar}H_p$), 134.1 ($C_{Ar}-CH_2$), 134.7 ($C_{Ar}-CH_2$), 136.8 ($C_{Py}H$), 146.0 (C_{Ar}), 149.0 ($C_{Py}H$), 154.0 (C_{Ar}), 154.6 (C_{Ar}), 157.9 (C_{Py}). IR (KBr): ν 3400 (H_2O), 3055, 3010, 2950, 1590, 1432, 760 cm^{-1}. Anal. Calcd for **2b**·H_2O: C, 79.12; H, 7.35; N, 3.70. Found: C, 79.37; H, 7.11; N, 4.40.

3b. $Cu(NCMe)_4PF_6$ (43 mg, 0.11 mmol) and **2b** (129 mg, 0.11 mmol) were mixed in dry THF (1 mL) under argon. After 3 h, a white precipitate was separated by centrifugation, washed with THF, and dried under vacuum. A second fraction of the product was obtained by precipitation of the mother liquor with pentane. After drying, 134 mg of a white solid was obtained (98%). Mp: 220 °C (decomp). ^{1}H NMR (400 MHz, CD_2Cl_2, 243 K, [**3b**] = 10 mM + 5 equiv of CH_3CN): δ −1.05 (3H, bs, CH_3CN_{in}), 1.35 (27H, s, *t*Bu), 1.99 (12H, s, CH_3CN_{out}), 2.94 (9H, s, OCH_3), 3.37 (6H, d, J = 15.0 Hz, $Ar-CH_{eq}$),), 4.27 (6H, d, J = 15.0 Hz, $Ar-CH_{ax}$), 5.51 (6H, s, $Py-\alpha CH_2$), 6.61 (9H, br, ArH_m and ArH_p), 7.29 (6H, s, ArH), 7.47 (3H, t, J = 5.5 Hz, PyH), 8.03 (6H, t, J = 7.5 Hz, PyH), 8.09 (6H, d, J = 7.0 Hz, PyH), 8.66 (3H, d, J = 4.3 Hz, PyH). IR (KBr): ν 3400 (H_2O), 3030, 2960, 1610, 1440, 845 (PF_6^-), 765, 555 (PF_6^-) cm^{-1}. Anal. Calcd for **3b**·3H_2O: C, 65.13; H, 6.34; N, 3.04. Found: C, 65.10; H, 6.07; N, 2.87.

3a. The same experimental procedure was applied to **2a** (126 mg, 0.098 mmol) and $Cu(MeCN)_4PF_6$ (36.5 mg, 0.098 m mol), to yield after drying 130 mg of **3a** (98%). Mp: 260 °C (decomp). ^{1}H NMR (400 MHz, CD_2Cl_2, 243 K, [**3a**] = 10 mM + 5.5 equiv of CH_3CN): δ −1.15 (3H, s, CH_3CN_{in}), 0.72 (27H, s, *t*Bu), 1.37 (27H, s, *t*Bu), 1.99 (15H, s, CH_3CN_{out}), 2.84 (9H, s, OCH_3), 3.34 (6H, d, J = 15.0 Hz,

$Ar-CH_{eq}$),), 4.26 (6H, d, $J = 15.0$ Hz, $Ar-CH_{ax}$), 5.50 (6H, s, $Py-\alpha CH_2$), 6.69 (6H, s, ArH), 7.34 (6H, s, ArH), 7.48 (3H, t, $J = 6.2$ Hz, PyH), 8.04 (6H, t, $J = 7.4$ Hz, PyH), 8.13 (6H, d, $J = 7.8$ Hz, PyH), 8.65 (3H, d, $J = 4.7$ Hz, PyH). IR (KBr): ν 3420 (H_2O), 2960, 1610, 1480, 845 (PF_6^-), 715, 555 (PF_6^-) cm^{-1}. Anal. Calcd for **3a**·$4H_2O$: C, 66.58; H, 7.26; N, 2.68. Found: C, 66.79; H, 7.05; N, 2.56.

Supporting Information Available: Details of molecular modeling and NMR spectroscopy for simulation experiments (PDF). This material is available free of charge via the Internet at http://pubs.acs.org.

JA0161958